EEG Signals And Machine Learning Based Facial Emotion Recognition

V Dyana Christilda[1], J Sharon Jixy Paul[2]
[1, 2] Dept of ECE
[1, 2] Vins Christian Women's College Of Engineering

Abstract- *Emotions are time varying affective phenomena that are elicited as a result of stimuli. Videos and movies in particular are made to elicit emotions in their audiences. Detecting the viewers' emotions instantaneously can be used to find the emotional traces of videos. Here, proposed approach in instantaneously detecting the emotions of video viewers' emotions from electroencephalogram (EEG) signals and facial expressions. A set of emotion inducing videos were shown to participants while their facial expressions and physiological responses were recorded. The expressed valence (negative to positive emotions) in the videos of participants' faces were annotated by five annotators. The stimuli videos were also continuously annotated on valence and arousal dimensions. Deep learning based neural network and Continuous Conditional Random Fields (CCRF) were utilized in detecting emotions automatically and continuously. Here found the results from facial expressions to be superior to the results from EEG signals. Analyzed the effect of the contamination of facial muscle activities on EEG signals and found that most of the emotionally valuable content in EEG features are as a result of this contamination. However, our statistical analysis showed that EEG signals still carry complementary information in presence of facial expressions.*

Keywords- electroencephalogram, facial expression, Deep learning, Continuous Conditional Random Fields

I. INTRODUCTION

Depression and anxiety disorders are highly prevalent worldwide. According to the World Health Organization (WHO), depression will become the fourth most serious mental health problem by 2020. Depression is often difficult to diagnose because it manifests itself in different ways. The diagnostic methodologies rely on patient self-report or on the clinical judgments of the severity of the symptoms. Both are rather subjective. Moreover, evaluations by clinicians depend on their expertise and the diagnosis method they employ. Several diagnosis methods are being used, such as the Diagnostic and Statistical Manual of Mental Disorders (DSM-IV), the Quick Inventory of Depressive Symptoms—Self Report (QIDS), the Beck Depression Inventory (BDI), the 10-item Montgomery–Asberg Depression Rating Scale (MADRS), the 9–item Patient Health Questionnaire (PHQ–9), and the PHQ–8. Recently, the affective computing community engaged signal processing, computer vision and machine learning approaches for analyzing verbal and nonverbal behavior of depressed patients. In, it has been suggested that dynamic activation of facial nonverbal behavior is crucial for measuring the severity of depression. Various systems for depression analysis have been proposed based on the observed non-verbal behaviors such as facial activities and expressions, head pose and movement, as well as gaze and eye activity.

This work focuses on building a framework for estimating a clinical depression-specific score, namely the Beck Depression Inventory (BDI) score, based on the analysis of facial expressions features. The purpose of this study was to extend our previous research on depression scale estimation focusing on facial expression analysis. This paper proposes a novel method that comprehensively models the variations in facial expressions and automatically predicts the BDI scale of depression. Local Binary Pattern (LBP), a non-parametric descriptor whose aim is to efficiently summarize the local structures of images, is the most widely used appearance features for facial image analysis. A face image can be considered as a composition of the micro-patterns described by LBP. One can build a LBP histogram computed over the whole face image. However, such a representation only encodes the occurrences of micro-patterns without any indication about their locations. To also consider the shape information of faces, Ahonen et al. proposed to divide face images into m local regions from which local LBP histograms can be extracted, and then to concatenate them into a single, spatially enhanced feature histogram. The resulting histogram encodes both the local texture and global shape of face images. Several variants of LBP have been successfully used for facial expression recognition as well depression diagnosis. To cope with dynamic textures and events across spatio-temporal dimensions of facial expressions, the classic LBP descriptor was extended to the local Binary Patterns from three orthogonal planes (LBPTOP), based on the concatenated LBP histograms computed from three orthogonal planes. The LBP-TOP has been used for depression analysis. Other variants, such as the Local Phase Quantisation from Three Orthogonal Planes (LPQ-TOP) and the local Gabor Binary

Patterns from Three Orthogonal Planes (LGBP-TOP), have also been used to capture the temporal dynamics of facial expression for depression diagnosis.

II. LITERATURE SURVEY

Automatically detecting facial expressions has become an increasingly important research area. In 2000, the Cohn-Kanade (CK) database was released for the purpose of promoting research into automatically detecting individual facial expressions. Since then, the CK database has become one of the most widely used test-beds for algorithm development and evaluation. As a consequence, the CK database has been used for both AU and emotion detection (even though labels for the latter have not been validated), comparison with benchmark algorithms is missing, and use of random subsets of the original database makes meta-analyses difficult. The target expression for each sequence is fully FACS coded and emotion labels have been revised and validated. In addition to this, non-posed sequences for several types of smiles and their associated metadata have been added. We present baseline results using Active Appearance Models (AAMs) and a linear support vector machine (SVM) classifier using a leaveone-out subject cross-validation for both AU and emotion detection for the posed data.

In the last decade, the research topic of automatic analysis of facial expressions has become a central topic in machine vision research. Nonetheless, there is a glaring lack of a comprehensive, readily accessible reference set of face images that could be used as a basis for benchmarks for efforts in the field. This lack of easily accessible, suitable, common testing resource forms the major impediment to comparing and extending the issues concerned with automatic facial expression analysis. In this paper, we discuss a number of issues that make the problem of creating a benchmark facial expression database difficult. We then present the MMI facial expression database, which includes more than 1500 samples of both static images and image sequences of faces in frontal and in profile view displaying various expressions of emotion, single and multiple facial muscle activation. It has been built as a Web-based direct-manipulation application, allowing easy access and easy search of the available images. This database represents the most comprehensive reference set of images for studies on facial expression analysis to date.

Facial expression recognition is to determine the emotional state of the face regardless of its identity. Most of the existing datasets for facial expressions are captured in a visible light spectrum. However, the visible light (VIS) can change with time and location, causing significant variations in appearance and texture. In this paper, we present a novel research on a dynamic facial expression recognition, using near-infrared (NIR) video sequences and LBP-TOP (Local binary patterns from three orthogonal planes) feature descriptors. NIR imaging combined with LBP-TOP features provide an illumination invariant description of face video sequences. Appearance and motion features in slices are used for expression classification, and for this, discriminative weights are learned from training examples. Furthermore, component-based facial features are presented to combine geometric and appearance information, providing an effective way for representing the facial expressions. Experimental results of facial expression recognition using a novel Oulu-CASIA NIR&VIS facial expression database, a support vector machine and sparse representation classifiers show good and robust results against illumination variations. This provides a baseline for future research on NIR-based facial expression recognition.

Facial expression is central to human experience, but most previous databases and studies are limited to posed facial behavior under controlled conditions. In this paper, A novel facial expression database, Real-world Affective Face Database (RAF-DB), which contains approximately 30000 facial images with uncontrolled poses and illumination from thousands of individuals of diverse ages and races has been presented. During the crowdsourcing annotation, each image is independently labeled by approximately 40 annotators. An expectation-maximization algorithm is developed to reliably estimate the emotion labels, which reveals that real-world faces often express compound or even mixture emotions. A cross-database study between RAF-DB and CK+ database further indicates that the action units of real-world emotions are much more diverse than, or even deviate from, those of laboratory-controlled emotions. To address the recognition of multi-modal expressions in the wild, we propose a new deep locality-preserving convolutional neural network (DLP-CNN) method that aims to enhance the discriminative power of deep features by preserving the locality closeness while maximizing the inter-class scatter. Benchmark experiments on 7-class basic expressions and 11-class compound expressions, as well as additional experiments on CK+, MMI, and SFEW 2.0 databases, show that the proposed DLP-CNN outperforms the state-of-the-art handcrafted features and deep learning-based methods for expression recognition in the wild. To promote further study, we have made the RAF database, benchmarks, and descriptor encodings publicly available to the research community.

Automated affective computing in the wild setting is a challenging problem in computer vision. Existing annotated databases of facial expressions in the wild are small and mostly cover discrete emotions (aka the categorical model).

There are very limited annotated facial databases for affective computing in the continuous dimensional model (e.g., valence and arousal). To meet this need, we collected, annotated, and prepared for public distribution a new database of facial emotions in the wild (called AffectNet). AffectNet contains more than 1,000,000 facial images from the Internet by querying three major search engines using 1250 emotion related keywords in six different languages. About half of the retrieved images were manually annotated for the presence of seven discrete facial expressions and the intensity of valence and arousal. AffectNet is by far the largest database of facial expression, valence, and arousal in the wild enabling research in automated facial expression recognition in two different emotion models. Two baseline deep neural networks are used to classify images in the categorical model and predict the intensity of valence and arousal. Various evaluation metrics show that our deep neural network baselines can perform better than conventional machine learning methods and off-the-shelf facial expression recognition systems.

III. PROPOSED SYSTEM

The Proposed system presents a framework towards estimating a clinical depression-specific score, namely the Beck Depression Inventory (BDI) score, based on the analysis of facial expressions features. To extract facial dynamic features, here propose a novel dynamic feature descriptor denoted as Median Robust Local Binary Patterns from Three Orthogonal Planes (MRLBP-TOP), which can capture both microstructure and macrostructure of facial appearance and dynamics. To aggregate the MRLBP-TOP over an image sequence, here propose a variant to the Fisher Vector (FV) encoding scheme, denoted as Dirichlet Process Fisher Vector (DPFV). DPFV adopts Dirichlet process Gaussian mixture models (DPGMM) to automatically learn the number of GMM mixtures and model parameters.

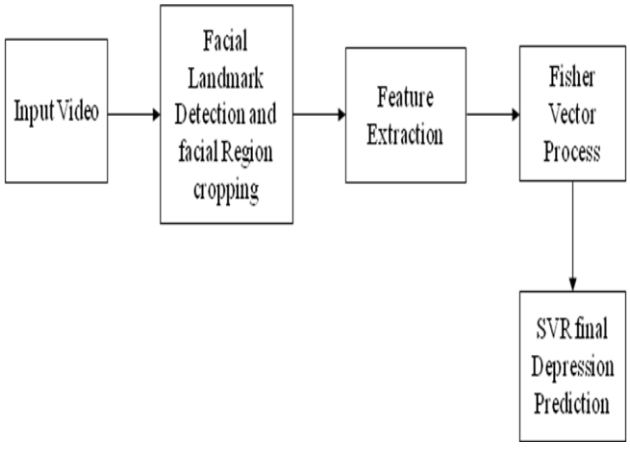

Fig 1 Proposed Block Diagram

Video Pre-processing

In our current implementation, the OpenFace toolbox is used for facial region detection and face alignment in each frame of the video sequence. Then to apply the MRLBPTOP, we cut the video sequence into many non-overlapping segments (sub-sequence). Several authors have studied the appropriate length of the sub-sequences for extracting reliable spatio-temporal features. In, sub-sequences of 20 frames were used. In, LPQ-TOP was applied to sequences of 60 frames. Here presents the extraction of spatiotemporal information patterns using the proposed MRLBPTOP, we conducted experiments using sub-sequences of 20, 60, and 90 frames, respectively. Sub-sequences of 20 frames gave the best results. These obtained empirical results are consistent with the theoretical analysis.

Analysis of facial expressions

A face tracker was employed to track 49 facial fiducia l points or landmarks. In this tracker, a regression model is used to detect the landmarks from features. It then calculates translational and scaling difference between the initial and true landmark locations. The main idea for feature tracking is to use supervised descent method (SDM) for the detection in each frame by using the landmark estimate of the previous frame. The model is trained with 66 landmarks, and provides the coordinates of 49 points in its output. The facial points were extracted after correcting the head pose. An affine transformation was found between a neutral face of each subject and an averaged face of all the subjects and all the tracked points of sequences were registered using that transformation. A reference point was generated by averaging the coordinates of the inner corners of eyes and nose landmarks. We assumed this reference point to be stationary. The distances of 38 point including eyebrows, eyes, and lips to the reference point were calculated and averaged to be used as features.

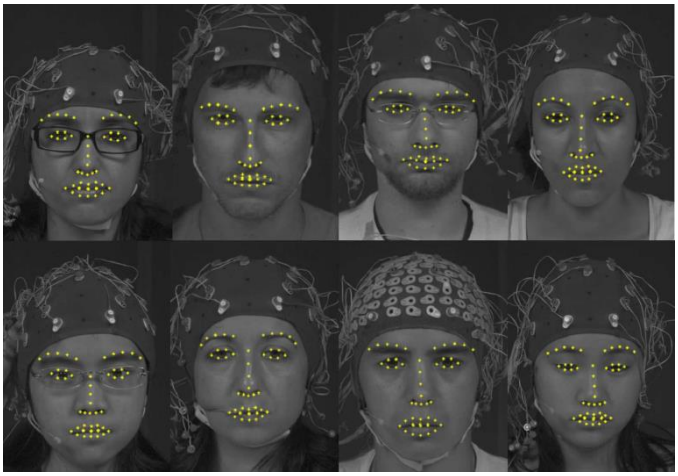

Examples of the recorded camera view including tracked facial points

Median Robust Local Binary Patterns

The LBP operator characterizes the spatial structure of a local image patch by encoding the differences between the pixel value of the central point and those of its neighbors, then forming a binary pattern by considering only the signs. Formally, given a pixel xc in the image, the basic LBP response is calculated by comparing its value with those of its P neighboring pixels ⟦{x_(R,P,n)}⟧_(n=0)^(P-1), evenly distributed on a circle of radius R centred at xc

$$LBP_{R,P}(x_c)\sum_{n=0}^{P-1} s(x_{R,P,n} - x_c)2^n, \qquad (3.1)$$

$$s_x = \begin{cases} 1, & if\ x \geq 0 \\ 0, & if\ x < 0 \end{cases}$$

Center pixel representation:

$$RELBP\_CI(x)_c = s(\emptyset(X_{c,w}) - \mu_w) \qquad (3.2)$$

where Xc,w denotes the local patch of size w×w centered at pixel xc and μw represents the mean of φ(Xc,w) over the whole image.

In our current implementation, we make use of the Center pixel (RELBP CI) and Neighbor (RELBP-NI) representations proposed.

The joint histogramming of RELBP CI and RELBP NI is used to represent a texture image. Details on the estimation of RELBP CI and RELBP NI.

MRLBP-TOP

To extend the MRELBP descriptors to the temporal domain, we follow the LBP-TOP algorithm, where the image sequence is regarded as a video volume from the perspective of three different stacks of planes, namely, the XY , XT and Y T planes. The XY plane provides the spatial domain information while the XT and Y T planes provide temporal information. The RELBP CI and RELBP NI features are extracted independently from three sets of orthogonal planes, considering the co-occurrence statistics in these three directions, and then they are stacked in a joint histogram. A similar approach has been adopted to extend the LPQ descriptor to the temporal domain, and use it for Action Unit detection.

Formally, to compute the MRLBP-TOP pattern of a pixel xc, we first extract the MRELBP, namely the RELBP CI and RELBP NI features, of xc on the XY plane with its PXY neighbors, followed by the MRELBP pattern on the XT plane with its PXT neighbors. Finally, the MRELBP pattern on the Y T plane is computed based on its PY T neighbors. This is repeated until all pixels in each frame have been considered. For each direction, the joint histogram of RELBP-CI and RELBP-NI is used to represent the texture image, and finally the three histograms are stacked into a single histogram to describe the dynamic texture of the video. In our proposed MRLBP-TOP, we follow the same approach and divide the input images of size 128 × 128 into 4 × 4 blocks, with time slices of 20 frames. As in many LBP applications, we also adopt the uniform encoding scheme.

The Fisher Vector (FV)

Recently, the Fisher Vector pooling method attracted increasing interest from the affective community for facial expression recognition, speech emotion recognition and depression analysis. It consists of two steps: creating a word vocabulary by clustering a set of local features, and encoding the local features to a global representation of the sequence using the Fisher kernel approach. sequence using the Fisher kernel approach.

Visual Vocabulary

In the first step, a dictionary is created using a GMM. Given a set of D-dimensional audio/visual feature vectors I = {x1, i = 1, ..., N} ∈ RN×D, where N represents the number of samples in the dataset, a GMM is fitted to the audio/visual features. Given K, the number of Gaussians, the GMM parameters can be learned using the Expectation Maximization (EM) algorithm. Let λ = (πj , μj , Σj , j = 1, ..., K), where πj , μj , Σj denote the mixing weight, mean vector, and covariance matrix of Gaussian j, respectively. Then the probability density function p(xi |λ) of a GMM.

Fisher Vector Coding

The essence of FV is the gradient of the log-likelihood of a set of features on the GMM with respect to its parameters. Here, perform a FV on different kinds of visual features extracted from a video segment. Let X = {xt, t = 1, ..., T} be a feature sequence of T frames. The local feature from one given frame of the video, denoted by xt, can be described by the gradient vector:

$$G_\lambda^x = \nabla logp(\text{xt}\,|\lambda) \qquad (3.8)$$

∇ denotes the gradient operator, and logp(xt|λ) the loglikelihood function.

The gradient of the log-likelihood describes the contribution of the parameters to the generation process of a feature sequence. In, a Fisher Kernel (FK) function on the gradient vector is used to measure the similarity between two feature vectors x and y, and which can be written as:

$$K(x, y) = G_\lambda^{x^T} F_\lambda^{-1} G_\lambda^y \qquad (3.9)$$

Fisher vectors (FV) are descriptors based on Fisher kernels. FV measures how samples are correctly fitted by a given generative model p(X|θ). Let X = {Xn}n=1:N, be a sample of N observations. The FV descriptor associated to X is the gradient of the sample log-likelihood with respect to the parameters θ of the generative model distribution, scaled by the inverse square root of the Fisher information matrix (FIM).

First, the gradient of the log-likelihood with respect to the model parameter vector θ, also known as the Fisher score (FS).

The gradient describes the direction in which parameters should be modified to best fit the data. In other words, the gradient of the log-likelihood with respect to a parameter describes the contribution of that parameter to the generation of a particular feature. A large value of this derivative is equivalent to a large deviation from the model, suggesting that the model does not correctly fit the data.

Support Vector Regression Analysis

A linear SVR with L2 regularization, from Liblinear library, was used and its hyper-parameters were found based on the lowest RMSE on the validation set. We used the validation sets in the process of training the LSTMRNN to avoid overfitting. The output of MLR on the validation set was used to train the CCRF. The trained CCRF was applied on the MLR output on the test set. The CCRF regularization hyper-parameters were chosen based on a grid search using the training set. The rest of the parameters were kept the same as.

Two fusion strategies were employed to fuse these two modalities. In the Feature Level Fusion (FLF), the features of these modalities were concatenated to form a larger feature vector before feeding them into models. In the Decision Level Fusion (DLF), the resulting estimation of valence scores from different modalities were averaged.

Here reported the averaged Pearson correlation to show the similarity between the detected curves and the annotations. Root-Mean-Squared Error (RMSE) is also reported to show how far the estimations were in average compared to the ground truth. RMSE penalizes the larger errors more than the smaller ones. Consistently, facial expressions outperformed EEG features. This might be as a result of the bias of the data set towards the trials with expressions. We could show that in this particular case unlike the work of Koelstara and Patras, facial expressions can outperform EEG signals for valence detection. It is worth noting that the facial landmark detector used in this study is a more recent landmark tracking technique compared to the one whereas the EEG features are identical. Moreover, compared to the previous work, we were using a different set of labels which were not based on self-reports. Finally, was a single trial classification study whereas here we are detecting emotions continuously.

A one sided Wilcoxon test showed that the difference between the performance of the decision level fusion compared to the results of a single modality facial expression analysis using LSTM-RNN was not significant. Therefore, we conclude that the fusion of EEG signals is not beneficial and the LSTM-RNN on a single modality, i.e., facial expressions, performed the best in this setting. Using the non-parametric Wilcoxon test, we found that the difference between correlations resulted from LSTMRNN and CCRF is not significant, however, RMSE is significantly lower for LSTM-RNN ($p < 1E-4$). Although, direct comparison of the performance is not possible with the other work due to the difference in the nature of the databases, the best achieved correlation is in the same range as the result of the winner of AVEC 2012 challenge, on valence and superior to the correlation value reported on valence in a more recent work. Unfortunately, the previous papers on this topic did not report the standard deviation of their results; thus its comparison was impossible. We have also tested the Bidirectional Long Short Term Recurrent Neural Networks (BLSTM-RNN), but their performance was inferior compared to the simpler LSTM-RNN for this task.

Here observed that positive emotions were easier to detect compared to the negative ones. Smiles are strong indicators of pleasantness of emotions and there are a large number of instances of smile in the current data set. It was also shown that smile detection has a high performance in spontaneous expression recognition. Our analysis on the face features also showed that most of the highly correlated features were the points on lips.

Expected Emotion Detection

If the goal of emotion detection is to identify the emotional highlight and emotional trace of videos, then the ground truth should reflect the expected emotions. For this reason, we repeated the same procedure for detecting the

expected emotion this time using both continuous arousal and valence labels given to the stimuli. When we annotated the stimuli directly here did not have the same limitation as annotating facial expressions that made annotating arousal impossible. This time, here only report the results of the best performing model, i.e., LSTM-RNN. Again the facial expressions results are superior to the EEG signals and fusion of two modalities do not outperform facial expressions. It is worth noting that even without the labels crated based on the expressions facial expressions outperform the EEG signals. The results are in average inferior to the results obtained using the expression-based labels. This might be as a result of different factors that here summarize as follows. Not all the viewers at all times feel the emotions that are expected; e.g., a person might have already watched a surprising moment in a movie scene and it is surprising to her for the second time. Often times here only express or feel high level of emotion or arousal only in the first moment of facing a stimulus; the emotional response usually decays afterward due to the habituation to the stimulus. Moreover, the personal and contextual factors, such as mood, fatigue and familiarity with the stimuli have effect on what here feel in response to videos. One solution to these problems can be to combine several users' responses. Multi-user fusion has been shown to achieve superior results in emotional profiling of videos using physiological signals compared to single user response.

In order to verify whether the model trained on annotations based on facial expression analyses can reflect on the case without any facial expressions. Here chose one of the videos with distinct emotional highlight moments, the church scene from "Love Actually", and took the EEG responses of the 13 participants who did not show any significant. Since these responses did not include any visible facial expressions, they were not used for the annotation procedure and were not in any form in our training data. Here extracted the power spectral features from their EEG responses and fed it into our models and averaged the output curves. That despite the fact that the participants did not express any facial expressions and likely did not have very strong emotions, the valence detected from their EEG responses covaries with the highlight moments and the valence trend in the video. The CCRF provides a smoother trace which matches better with the overall trend compared to the other methods. The frames corresponding to three different moments. The first one, at 20 seconds, is during the marriage ceremony. The second and third frames are the surprising and joyful moments when the participants bring their musical instruments in sight and start playing a romantic song unexpectedly

IV. SCREEN SHOTS

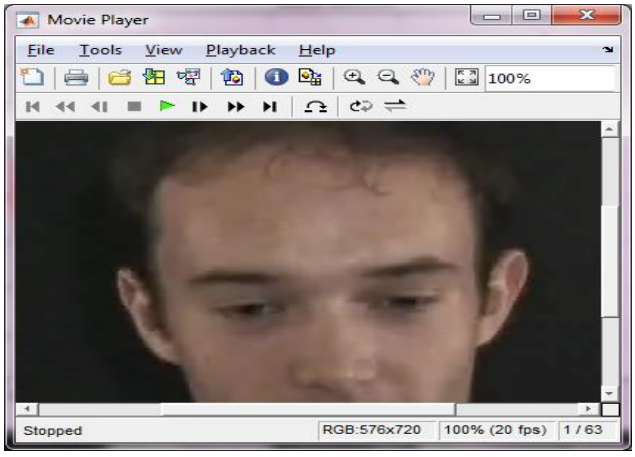

Input Video

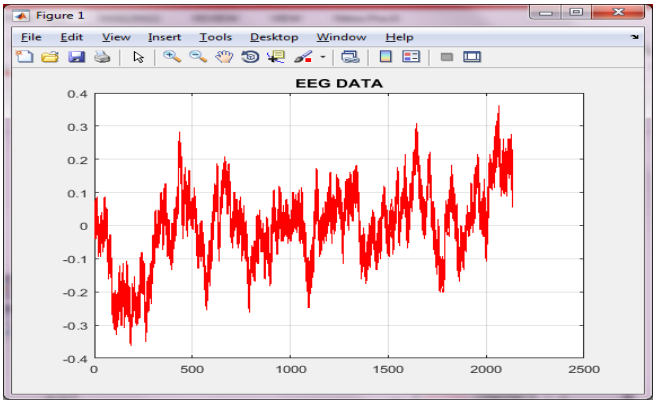

EEG Data

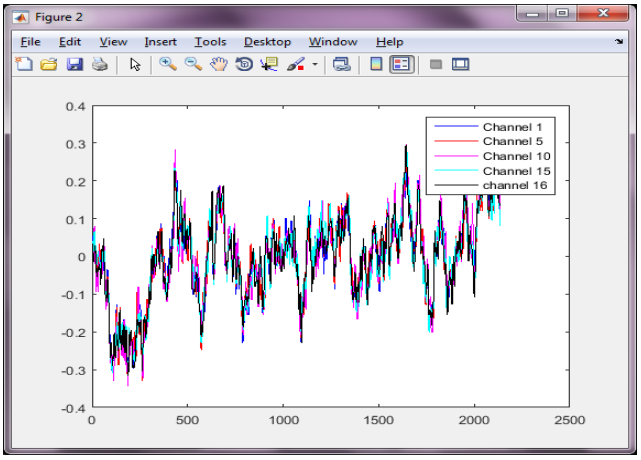

EEG Data channel waveform

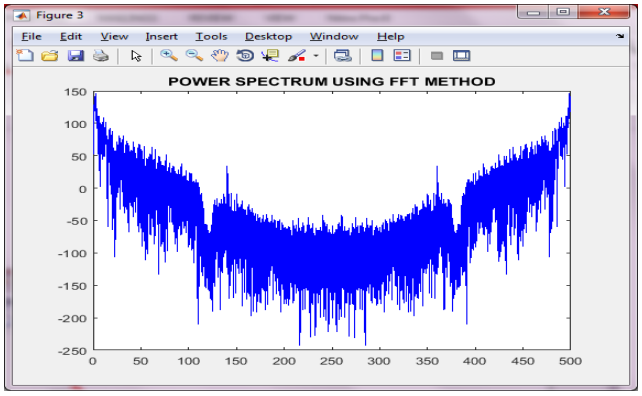

Simulation waveform for power spectrum using FFT method

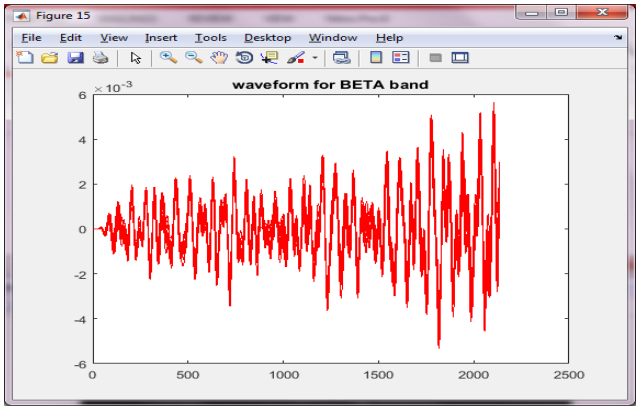

Simulation waveform for BETA band

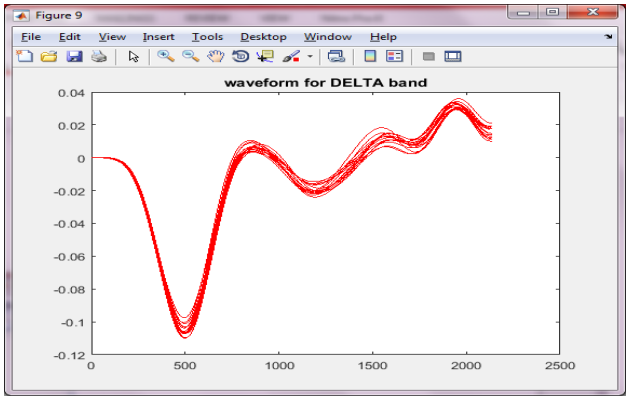

Simulation waveform for the DELTA band

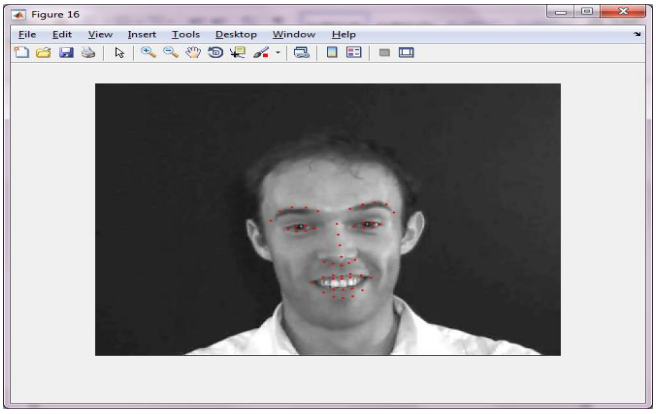

Simulation waveform

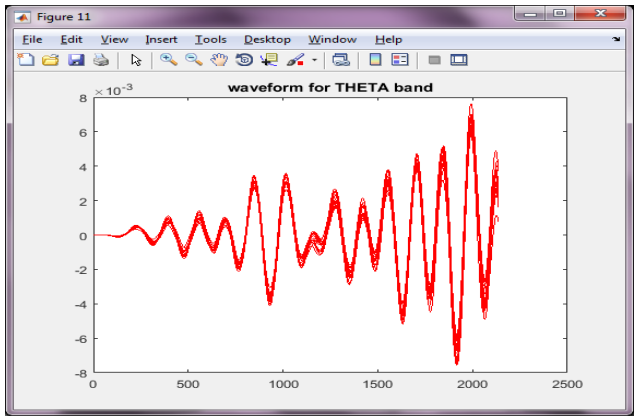

Simulation waveform for THETA band

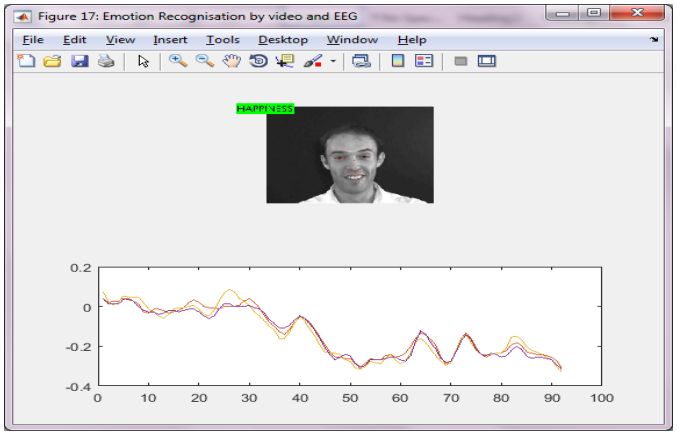

Classification Result

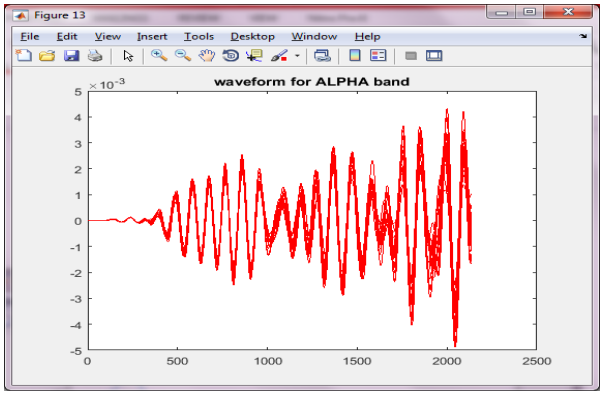

Simulation waveform for ALPHA band

V. CONCLUSION

Thus, a novel approach for capturing temporal facial expressions dynamics, using the Median Robust Local Binary Patterns from Three Orthogonal Planes as appearance descriptor of facial expressions. The continuous detection of valence using EEG signals and facial expressions. Promising results were obtained from EEG signals and facial expressions. The results from the statistical test on the linear mixed effect model showed that EEG modality carries useful information for detecting valence. The results of detecting the

labeled stimuli again demonstrated that facial expressions had superior performance compared to the EEG signals for emotion detection. Moreover, proposed the Dirichlet Process Fisher Vector (DPFV) to learn richer and more compact and intermediate representations of the MRLBP-TOP features. Finally, demonstrated that our proposed framework outperforms state-of-the-art methods.

REFERENCES

[1] Chu R., Liao S., Han Y., Sun Z., Li S. Z and Tan T., (2007), "Fusion of face and palmprint for personal identification based on ordinal features," in Proc. IEEE Conf. Comput. Vis. Pattern Recognit. (CVPR), Jun, pp. 1–2.

[2] Dai J, Zhou J, " Multifeature based high resolution palmprint recognition". IEEE Transaction on pattern analysis,

[3] Fei L., Lu G., Jia W., Teng S., Zhang D., (2018), "Feature Extraction Methods for Palmprint Recognition: A Survey and Evaluation," IEEE Transactions on Systems, Man, and Cybernetics: Systems, DOI: 10.1109/TSMC.2018.2795609, pp.1-18.

[4] Fei L., Lu G., Jia W., Wen J., Zhang D., (2018), "Complete Binary Representation for 3-D Palmprint Recognition", IEEE Transactions on Instrumentation and Measurement, vol.17, no.12, pp.2761-2771.

[5] Huang D. S., Jia W and Zhang D., (2008), "Palmprint verification based on principal lines," Pattern Recognit., vol. 41, no. 4, pp. 1316–1328, Apr.

[6] Kong A.W. K and Zhang D., (2004), "Competitive coding scheme for palmprint verification," in Proc. 17th Int. Conf. Pattern Recognit.,vol.1. Aug, pp. 520–523.

[7] Kong W. K., Zhang D and Kamel M. S., (2009), "A survey of palmprint recognition," Pattern Recognit., vol. 42, no. 7, pp. 1408–1418, Jul.

[8] Kong, D. Zhang, and M. Kamel, (2006), "Palmprint identification using feature-level fusion," Pattern Recognit., vol. 39, no. 3, pp. 478–487, Mar.

[9] Palma D., Montessoro P. L., Giordano G., Blanchini F., (2017), "Biometric Palmprint Verification: A Dynamical System Approach," IEEE Transactions on Systems, Man, and Cybernetics: Systems, vol.99, pp.1- 12.

[10] Rida I., Maadeed S. A., Mahmood A., Bouridane A., Bakshi S., (2018), "Palmprint identification using an ensemble of sparse representations," IEEE ACCESS, vol.6, no.1, pp.3241-3248.

[11] Zhang D., Kong W. K, You J., Wong L. M., (2003), "Online Palmprint Identification," IEEE Transactions on Pattern Analysis and Machine Intelligence, vol.25, no.9, pp.1041-1050.

[12] Zhang D., Kong W.K., You J and Wong M., (2003), "Online palmprint identification," IEEE Trans. Pattern Anal. Mach. Intell., vol. 25, no. 9, pp. 1041–1050, Sep.

[13] Zhang D., Song F., Xu Y and Lang Z., (2009), "Advanced pattern recognition technologies with applications to biometrics," Med. Inf. Sci. Ref.,Jan, pp. 1–384.

[14] Zhang D., Zuo W and Yue F., (2012), "A comparative study of palmprint recognition algorithms," ACM Comput. Surv., vol. 44, no. 1, pp. 1–37, Jan.

[15] Zhang L., Li L., Yang A., Shen Y., Yang M., (2017), "Towards contactless palmprint recognition: A novel device, a new benchmark, and a collaborative representation based identification approach," Pattern Recognition, vol.69, pp.199-212.